Primary cosmic ray chemical composition in the energy region around 10^{16} eV investigated by means of γ-hadron families.

Maia Kalmakhelidze, Nina Roinishvili, Manana Svanidze[†]

E.Andronikashvili Institute of Physics,

Academy of Sciences of the Georgian Republic,

Tamarashvili 6, Tbilisi, Georgian Republic, 380077.

(Dated: February 7, 2008)

Primary Cosmic Ray Chemical Composition is investigated in energy region close to 10^{16} eV. Studies are based on comparisons of γ-hadron families observed by Pamir and Pamir-Chacaltaya Collaboration, with families generated by means of quasi-scaling model MC0. It is shown, that all characteristics of observed families, including their intensity, are in a very good agreement with simulated event properties at the normal chemical composition and are in disagreement at heavy dominant compositions. Code CORSICA with VENUS and DPM models also contradicts with experimental data of families. One- and multi-dimensional methods of recognition of Fe-like families is worked up and approved. They are based on family characteristics sensitive to atomic number of induced nuclei and are not correlated between each others. It is shown that the fraction of Fe-like families is consistent with the normal chemical composition and strongly contradicts to heavy dominant ones. The success of MC0 model, in description of families properties, is due to large inelasticity coefficient of soft interactions at superhigh energies.

1. Introduction

The investigation of Primary Cosmic Ray (PCR) Chemical Composition(CC) is one of the key problem for understanding of PCR origin, properties of radiation sources and interstellar or extra Galaxy space, which PCR passes from a source to the Earth. CC is well investigated up to energy 10^{12}eV. By direct methods CC is studied up to energy 10^{15} eV [1, 2, 3]. However the reliability of results of these work is not great, since they base on small statistics. At larger energies sources of the information about CC is Extensive Air Showers (EAS) or families of γ-quanta and hadrons, registered by X-ray emulsion chambers . Despite of long-term researches the results are very inconsistent. The statements concerning CC swing from so-called normal [4, 5] and even with proton dominant [6] to heavy [6, 7] and superheavy [8] compositions. The appropriate data with the references are brought in Table I.

Whereas the knowledge of CC in the region 10^{15} - 10^{16} eV is especially important as a complete spectrum of PCR in this area has a "knee".

The reason could be either spectrum bend of PCR (due to decrement some the component from PCR content) or change properties of inelastic interaction between cosmic ray particles and Earth's atmosphere nucleus at these energies [1, 9].

The present work is devoted to research of PCR CC in the energy region directly after bend of a energy spectrum of PCR. The γ-hadron families are registered and processed by Pamir and Pamir-Chacaltaya Collaborations. The characteristic of the families are used for this task.

Running ahead we shall notice, that efficiency of families generated by a nucleus, ϵ_A, strongly depends on their atomic number decreasing with increase of A. Therefore the chemical composition of families differs much from CC of PCR:

$$f_A = \epsilon_A \times C_A / \Sigma(\epsilon_A \times C_A) \tag{1}$$

For comparison see Table I and II.

Table II explains the main difficulty of investigation of PCR CC based on data about families. Even if characteristics of families induced by heavy nuclei strongly differ from that

TABLE I: Used chemical composition of PCR at $E_0 = 10^{15}$ eV , $C_A\%$

.

Composition	P	He	CNO	SiMg	Fe	$\langle \ln A \rangle$
Normal[4, 5]	40	20	10	10	20	1.7
Heavy [6, 7]	15	10	17	0	58	3.0
Superheavy [8]	7	5	12	6	70	3.4

TABLE II: Chemical composition of families, $f_A\%$

.

Composition	P	He	CNO	SiMg	Fe
Normal [4, 5]	75.	16.6	3.2	2.4	2.8
Heavy [6, 7]	56.	16.6	11.	0	16.4
Superveavy[8]	40.	12.6	12.	4.4	31.

of proton families, influence of the former to the average characteristics of families is not great, since CC of families is strongly enriched by protons. Even at heavy composition of PCR, in which iron makes about 60%, they provide only 16.4% of families. How Table II is received and what is possible to make for the analysis of PCR CC by data on families will be discussed in the subsequent sections.

A γ-hadron family is a result of Nuclear Electromagnetic Cascade (NEC) developed in the Atmosphere after interaction of PCR particles with nuclei of air in the top part of the Atmosphere. This process is very complex, multistep and branching. Therefore to get information from characteristics of families one needs a comparison with Monte-Carlo calculation based on some mode including both nuclear and electromagnetic cascades.

Not less than ten of such models [5, 10, 11, 12, 13, 14, 15, 16, 17] were developed up to day. All recent models of nuclear interactions [5, 15] are quasi-scaling type. Scaling is violated in pionisation region. But this almost not influences properties of families, since they are formed mostly by particles from fragmentation region. Scaling is violated a little in

fragmentation region as long as the interaction of a primary particle of PCR occurs not with a nucleus of air. All these models are in the agreement with accelerator's experiments and represent extrapolation of their properties to superhigh energies. They differ insignificantly in details of the interaction: in quantity of use flavors of secondary particles, in a way of inclusion of diffraction processes and production of jets with large transverse momentum.

In the majority of quasi-scaling models the intensity of families at normal chemical composition is 2-4 times more then observed [18, 19, 20, 21]. A dilemma is arisen: either admit scaling violation in the fragmentation region or assume heavy composition of PCR [7, 8]. This explains the appearance of simulations based on compositions with dominance of heavy elements (Table I). By this point of view paper[21] is especially interesting as different possible decisions of the dilemma are proposed in it.

MC0 model [5] is used in the present work for the analysis of data observed with the help of X-ray emulsion chambers. The Model is based on the theory of quark-glion strings. Diffraction processes, generation of jets with large transverse momentum, production of strange and charm particles are included in it. The important peculiarity of MC0 is a large inelasticity coefficient. Details of the model are described in [5].

Let us note, that for to day the most popular is code CORSIKA with some variants of strong interaction model. Comparisons of MC0 predictions with results of CORSIKA calculations in variants DPM and VENUS were made in work [22, 23, 24]. There was shown that MC0 predicts faster absorption of hadron component than both variants of CORSIKA. As it will be apparent from the following fast absorption of hadron component provides the agreement of MC0 model with observed intensity of γ-families. Model MC0 and CORSIKA differs also in the average characteristics of families. The characteristics in MC0 are closer to the experimental data than in CORSIKA. This explains a choice of MC0 as base for the subsequent analysis.

With the help of MC0 model nuclear-electromagnetic cascades in the Atmosphere generated by various nuclei were simulated at power like energy spectrum. Index of integral energy spectra of PCR, γ, for all nuclei was also simulated. γ=1.7 for energies less then

3×10^{15} eV and γ=2.2 below the "knee" were input in this case.

There are 6 sections in the present paper. Besides Introduction (sec.1) and conclusion (sec.6) it contains 4 main parts each of which are subdivided on two subsections concerning experimental and modeling considerations. Section 2 is dealing with the problem concerning intensity of families at the altitude of Pamir. Observed (subsec.2.1) and predicted (subsec.2.2) intensities are considered there. In the next two subsections (3.1 and 3.2) properties of experimental and simulated families are described. In subsection 4.1 the consistency of the model with the experimental data is discussed while in subsection 4.2 this subject is analyzed with the account of possible systematic errors in the experiment. One- and multi-dimensional methods of recognition of families generated by iron are elaborated and applied to the Pamir data. This is done in subsections 5.1 and 5.2. 5.1 is a short review of the situation but 5.2 is an original investigation. In the last section the results are summarized.

2. Intensity of γ-hadron families .

In the next two subsections intensity of γ-hadron families are studied from experimental and theoretical point of view. In the end of subsection 2.2 the results are compared and a solution of the dilemma, heavy composition or scaling violation in the fragmentation region, is found. In the frame of quasi-scaling model good agreement between observed and predicted intensity at the normal chemical composition is achieved. This is due to large inelasticity coefficient in MCO model.

2.1 Intensity of γ-hadron families, Pamir experiment.

A group of γ-quanta (true γ and also e^+, e^-) and hadrons (π^+, π^-, n, p...) produced in NEC by interaction of a PCR particle with a nucleus of air is called the γ-hadron family. In this paper we analyze families satisfying the following conditions:

$$100TeV \leq \Sigma E_\gamma \leq 1000TeV,$$
$$n_\gamma \geq 10, \quad E_\gamma, E_h^\gamma \geq 4TeV, \quad 1cm < R_\gamma < 15cm \tag{2}$$

In (2) E_h^γ, E_γ is visible energy of a hadron or a γ-quantum, R_γ - average radius of the family count off from its energy weighed center.

Only γ-quanta seated at distance less than 15cm from the energy-weighted centre of a family are included in it.

So-called, aggregation procedure was used at processing of families. It consists of taking a pair of γ-quanta ($\gamma_i\gamma_j$), being at distance R_{ij} smaller then 0.15 mm, as one with $E_\gamma = E_{\gamma_i} + E_{\gamma_j}$. The majority of such quanta actually combine their spots of darkness and the scanner's eye apprehends them as one. The rest we unite by the aggregation procedure as in real so in simulated families. Thus all γ-quanta with R_{ij} <0.15 mm are united.

Let us pay attention to the condition R_γ <1cm. This selection condition is applied to families for the first time. It is connected with two circumstances. On the one hand the characteristics of families with R_γ <1cm are strongly distorted by process of formation of dark spots on X-ray film of emulsion chamber. A large part of them are overlapped, some of them are almost completely united. These peculiarities of the registration are difficult to reproduce in simulated families. Therefore we prefer to exclude them from consideration. The same reasons concern to families with $\Sigma E_\gamma \geq 1000$ TeV. In their central part there are very narrow bunches of γ-quanta which are also difficult to separate. On the other hand it was noticed [25] that the relative part of narrow families in experiment is more than in simulations (Fig. 1a) and their properties differ from properties of the other families. For example, families with R_γ <1cm in experiment are almost away of hadrons and their spectrum of E_γ is very similar to the spectrum of E_γ in purely electromagnetic cascades. It also indicates that group of families with R_γ <1cm is preferable to exclude from the analysis. Figure 1b shows that after exclusion of events with R_γ <1cm experimental and simulated distributions of R_γ become closer.

Intensity of γ-hardon families [10] at Pamir level (4370m above sea, 596 gr/cm^2) without condition $R_\gamma \geq$1cm is equal to

$$(0.69 \pm 0.15) m^{-2} year^{-1} str^{-1} \tag{3}$$

Error bars include statistical and possible systematically uncertainties.

Total number of families studied in the present work including narrow events (R_γ <1 cm) equals to 226. Without them it becomes 174.

Thus the experimental intensity of families satisfying the criterion (2) is

$$I_{exp} = (0.69 \pm 0.15) \times 174/226 = (0.53 \pm 0.12) m^{-2} year^{-1} str^{-1} \tag{4}$$

2.2 Intensity of γ-hadron families , MC0-model.

The vertical intensity of γ-hadron families can be expressed as:

$$I^v_{fam} = \Sigma[I_A(E \geq E_0) \times \epsilon_A(E \geq E_0) \times \Omega_0/\Omega^{fam}_A] \tag{5}$$

$I_A(E \geq E_0)$ - is an intensity of nuclei with atomic number A and energy $E \geq E_0$,

$\epsilon_A(E \geq E_0)$ - is an efficiency of families production satisfying the given conditions.

In turn

$$\epsilon_A = N^A_{fam}/N_A(E \geq E_0) \tag{6}$$

$N_A(E \geq E_0)$ is the number of NEC, induced by a primary particle with atomic number A and N^{fam}_A - number of families, which they have produced.

It is convenient to have I_A in percentage of I, i.e. to normalize it on total intensity:

$$C_A = I_A/I \tag{7}$$

In (5) Ω_0 and Ω_{fam} are solid angles for primary particles and families:

$$\Omega_0 = 2\pi \qquad \Omega_{fam} = 2\pi/(1 + T/\lambda_{att}) \tag{8}$$

Here T is air pressure at the altitude of installation's exposition (600 gr/cm^2 for Pamir) and λ_{att} is attenuation mean free path of families.

As one can see from (5-8) at determination of calculated intensity model defines only ϵ_A (efficiency of production), whereas C_A and the index of energy spectra of nuclei are set by assumed chemical composition. Simulation calculations have shown that λ_{att} is independent

of A in the limit of their errors and equals to $75 \pm 6\ gr\ cm^{-2}$. This value is in a good agreement with the experimental figure $\lambda_{att}^{exp} = 78 \pm 4\ grcm^{-2}$ [10].

Vertical intensity for all particles of PCR

$$I^v(E \geq E_0) = \Sigma I_A^v(E \geq E_0) \tag{9}$$

is estimated up to very high energy. It is customary to use empirical expression for $\Sigma I_A^v(E \geq E_0)$ given in article [4]. We also use it but change the integral energy spectra index -1.6 accepted in [4] to more recent value γ=-1.7. As a result we have:

$I^v(E > 10^{15}eV) = (50 \pm 20)\ m^{-2}year^{-1}srt^{-1}$

The new figure for differential vertical intensity is obtained in [1]. It gives for $I^v(E > 10^{15})$:

$I^v(E > 10^{15}eV) = (47 \pm 12)\ m^{-2}year^{-1}srt^{-1}$.

Combining these two results we use the following value for I^v:

$$I(E > 10^{15}eV) = (50 \pm 15)\ m^{-2}year^{-1}srt^{-1} \tag{10}$$

Efficiencies obtained by means of MC0 model for different nuclei are brought in Table III.

$N_A^{sim}(E \geq E_0)$ are given in the first row of TableIII. $N_A^{sim}(E \geq E_0)$ are actual number of cascades simulated isotropically over zenithal angle interval from 0^o up to 43^o. For light nuclei (P, He) $E_0 = 10^{15}$ eV. In the case of groups of nuclei CNO and $SiMg$ and also for Fe nuclei the minimal primary energy was put as

$$E_0^A = A^{0.5} \times 10^{15}eV \tag{11}$$

Such a choice of Θ_{max} and E_0 is determined by the fact that nuclei with energy less than specified E_0 and $\Theta > \Theta_{max}$ form no more than 2% from total number of families.

In the second row of TableIII corrected number of cascades $N_A(E \geq 10^{15}$ eV) are brought.

$$N_A(E \geq 10^{15}eV) = N_A^{sim}/(1 - cos43^o)/(E_0^A)^{1.7} \tag{12}$$

TABLE III: Efficiency of family production by different nuclei, ϵ_A, and average energy of nuclei, responsible for them, E_A.

	P	He	CNO	SiMg	Fe	P(γ=-2.2)
$N_A^{sim} \times 10^3$	63.6	87	30	20	30	62
$N_A \times 10^3$	237	324	912	1113	3450	231
N_A^{fam}	682	416	461	434	756	409
$\epsilon_A \times 100$	$.29 \pm .01$	$.13 \pm .01$	$.051 \pm .003$	$.038 \pm .003$	$.022 \pm .001$	$.18 \pm .01$
E_A,PeV	15.	29.	53.	66.	80.	9.

In Table III N_A^{fam} is number of families generated by the given nucleus and ϵ_A - efficiency of their production. Data for protons having above the "knee" ($E_{knee} = 3 \times 10^{15}$ eV) spectral index γ = -2.2 are given in the last column of Table III.

Figures given in Tables I and III allow to determine efficiency of family production, ϵ, at the given chemical composition, C_A, and energy spectrum index, γ. Further on one can get predicted vertical intensity of families, I_{fam}^v , average energy of primary nuclei responsible for families, E_{fam}, and average $\ln A$.

$$\epsilon = \Sigma(C_A \times \epsilon_A)/\Sigma C_A \tag{13}$$

$$I_{fam}^v = I_0^v \Sigma[C_A \times \epsilon_A \times (1 + T/\lambda_{att}^A)] \tag{14}$$

$$E_{fam} = \Sigma(C_A \times \epsilon_A \times E_A)/\Sigma(C_A \times \epsilon_A) \tag{15}$$

$$\langle \ln A \rangle = \Sigma(C_A \times \ln A)/\Sigma C_A \tag{16}$$

The values C_A and $\langle \ln A \rangle$ for investigated CC are given in Table I (section 1), ϵ_A and E_A - in Table III. Parameters calculated by (13, 14, 15) are brought in Table IV. Dependencies of family production efficiency on $\ln A$ for pure nuclei and on $\langle \ln A \rangle$ for various chemical compositions are shown in Figure 2a. Predicted intensities of families at different chemical

compositions are brought in Figure 2b. In Figure 2b the strip limited by broken lines corresponds to region allowed by the experiment. Table IV and Figure 2b show that only normal compositions (NC) with γ = -1.7 for all nuclei and NC with γ = - 1.7 for all components except protons (γ_P = - 2.2 for energy more then $E_0 = 3\times10^{15}$ eV) are consistent with the experimental intensity of γ-hadron families. The heavy compositions [7, 8] predict intensity of families essentially less then the experimental value. Let us note, that an account of possible systematic errors in energy measurement of γ-quanta and hadrons only strengthen reliability of the conclusions. Discussions in subsection 4.2 show that predicted intensity at normal composition become $(0.58 \pm 0.18)\ m^{-2}year^{-1}srt^{-1}$ and at heavy composition - $(0.25 \pm 0.08)\ m^{-2}year^{-1}srt^{-1}$ after the account for systematically errors.

Thus we come to the following conclusions:

- Model MC0 eliminates the dilemma: heavy chemical composition or strong scaling violation in fragmentation region. In framework of quasi-scaling models the agreement between experimental and calculated intensity of families at normal chemical composition is managed. This progress is due to rather large inelasticity coefficient in MC0 model.

- Heavy and superheavy chemical compositions in MC0 model give too low values of family's intensity.

One more result of simulations should be underline. Table III indicates that the average energy of nuclei responsible to family's production is about 10^{16} eV. Therefore the conclusion following from our investigations of families correspond to the energy interval just above the "knee" of energy spectra of PCR.

3. Characteristics of γ-hadron families.

γ-hadron families are characterized by a number of measured parameters. Their definitions and descriptions are given in the next two subsections. Again in the first one experimental questions and problems connected with measurement of parameters are discussed.

TABLE IV: Calculated parameters (see the text)

.

Composition	$\epsilon \times 100$	I_{fam}	E_{fam},PeV
Normal[4]	0.16	$0.71 \pm .22$	22.
Heavy[6, 7]	0.076	$0.35 \pm .11$	32.
Superheavy[8]	0.051	$0.23 \pm .07$	45.
Normal($\gamma_p = -2.2$)	0.11	$0.49 \pm .15$	17.

The results of calculations and some specific circumstances are analyzed in the second subsection. On the base of simulated events parameters sensitive to atomic number of incident nucleus are found out. Short conclusions about agreement between experimental and calculated values of parameters at the normal composition are given in the end of subsection 3.2.

3.1 Characteristics of γ-hadron families, Pamir experiment.

γ-hadron families are characterized by number of measuring parameters. Conditionally they can be divided into 4 classes:

- 1. Characteristics of γ-quanta related to energy: $n_\gamma, \Sigma E_\gamma, \Sigma E_\gamma/n_\gamma$.

  n_γ - number of γ-quanta, ΣE_γ - total energy of γ-quanta.

- 2. Spatial characteristics of γ-quanta: $R_\gamma, E_\gamma R_\gamma, R_\gamma^E = \Sigma E_\gamma R_\gamma / E_\gamma$ and d.

  R_γ - radius of a family (average distance from the center of the family), $E_\gamma R_\gamma$ - average product $E_\gamma R_\gamma$, R_γ^E average radius weighted by energy. Parameter $d = n_{in}/n_{obs}$ is defined as the ratio of the number of initial γ-quanta, n_{in}, to the number of observed γ-quanta, $n_{obs} = n_\gamma$. An initial γ-quantum is responsible for a narrow group of spots on an X-ray film, which are the result of an electromagnetic cascade induced by it in the Atmosphere. Observed dark spots being on a small distance, R_{ij}, from each

TABLE V: Average values of parameters, P, their statistical errors, σ_P, in experimental families and sensitivity of parameters, S.

	n_h	R_γ(cm)	R_γ^E	$E_\gamma R_\gamma$	d	q_n	q_E
P	3.1	2.8	2.4	27.	.63	.11	.14
σ_P	0.3	0.1	0.1	2.0	.01	.01	.01
S	1.38	1.33	1.26	1.04	.96	.65	.60

other are combined into one initial γ-quantum, if $R_{ij}/(1/E_i + 1/E_j) < 10\ TeV \times mm$. Using this algorithm, called decascading procedure, the number of initial γ-quanta is determined.

- 3. Characteristics of hadrons related to energy: n_h, ΣE_h^γ,

  $q_E = \Sigma E_h^\gamma/(\Sigma E^\gamma, +\Sigma E_h^\gamma)$, $q_n = n_\gamma/(n_\gamma + n_h)$

  n_h - number of hadrons, E_h^γ - energy transferred by a hadron into soft component (visible energy of a hadron), ΣE_h^γ - total visible energy of hadrons, q_E - fraction of energy carried by hadron component of a family and q_n - fraction of hadrons in total multiplicity.

- 4. Spatial characteristics of hadrons: $R_h, E_h^\gamma R_h$ and etc. Let us note, that the last characteristics are not examined in this work, since the number of hadrons is, as a rule, small and consequently their spatial characteristics have very wide fluctuations.

Parameters belonging to a given class are subject to common systematic errors. In the 1-st class they are determined by errors in energy measurement of γ-quanta. For energy from 4 up to 50 TeV the relative error is about 20%. The effects of saturation of darkness and the overlapping of spots appeared for larger energies. Whenever possible these effects are taking into account during primary processes of families. At the next stage of treatment, γ-quanta being on distance $R_{ij} < 0.15$ mm are united in one and only families with $\Sigma E_\gamma < 1000$ TeV and $R_\gamma > 1$cm are included into analysis (see subsection 2.1). As it seems these restrictions

eliminate the main part of systematic errors of the 1-st class parameters. This question is discussed in more detail in subsection 4.2. Complexities in determination of spatial characteristics (the 2-nd class) were already discussed in subsection2.1. We should remind that aggregation of quanta with $R_{ij} < 0.15$ mm and exclusion of families with $R_\gamma < 1$ cm from analysis set aside most difficulties. Main uncertainties of the 3-rd class's parameters are connected with determination of visible energy of a hadron, E_h^γ, based on its darkness. Due to two reason the situation here is easier than with γ-quanta: the saturation of a darkness comes later, as distribution of density is more flat in case of hadron and overlapping is not present, since average distance between hadrons is much more than between γ-quanta. However, the relation between visible energy and density of darkness for hadron are investigated not so carefully as for γ-quanta [26]. This complexity will be discussed in subsection3.2 in connection with determination of visible energy of hadrons in simulated families. Average values of parameters of the experimental families with their statistical errors are given in Table V.

Sensitivity of a parameter to atomic number of primary particle is defined as:

$$S = (< P_{Fe} > - < P_P >)/D_P \tag{17}$$

$< P_{Fe} >$ - is an average value of the given parameter for families induced by Fe, $< P_P >$ - the same for families induced by protons, D_P - dissipation of a parameter for primary proton. S was calculated by means of simulated families for primary protons and iron. Let us note, that all parameters are defined in such a way that $< P_P >$ is less than $< P_{Fe} >$. For this purpose in two cases it was necessary to depart from initial definitions of parameters. Parameter d was introduced for the first time in work [27] as the ratio $d = n_{obs}/n_{in}$. We have redefined it by replacing $d \to 1/d$. Parameter q_E, was introduced in work [28] as $q_E = \Sigma E_\gamma/(\Sigma E^\gamma, +\Sigma E_h^\gamma)$. We transformed it as $q_E \to 1 - q_E$. In Table V parameters are brought in order of decrease of their sensitivity. Characteristics of families with $S < 0.5$ are not given there. At a research of chemical composition they can be only harmful. Not having sensitivity they are useless but the systematic errors in them can enter distortions

into final results. Distributions of two parameters sensitive (R_γ) and not sensitive (n_γ) to atomic number of a primary nuclei are demonstrated in Figures 3a and 3b.

3.2 Characteristics of γ-hadron families, MC0-model.

The average value of a given parameter of families, P, at certain chemical composition can be expressed by a formula:

$$P = \Sigma(C_A \times \epsilon_A \times P_A)/\Sigma(C_A \times \epsilon_A) \tag{18}$$

where P_A is an average value of the given parameter in families generated by a nucleus with atomic number A; C_A - a fraction of nuclei A at the given chemical composition of PCR; ϵ_A - an efficiency of family production by nuclei A with the energy above 10^{15}eV. As above, the model determines values P_A and ϵ_A, whereas CC and the power index of energy spectra of nuclei A are set as an input of simulations. It was already noted that all procedures used at selection and processing of experimental data were applied to simulated families. Peculiarity of simulated events is a modelling of hadron registration in X-ray emulsion chamber and determination of energy transferred by it into the soft component, $E_\gamma^h = K_\gamma \times E_h$. A hadron is registered by X-ray film if it has interacted in the chamber and energy transferred by it, E_γ^h, is more than threshold value - 4 TeV. The probability of hadron interaction and factor K_γ is determined by a design of X-ray emulsion chamber. For Pamir carbon chambers special investigations [29] have shown that the probability of interaction is about 0.7 and K_γ has a distribution, $f(K_\gamma)$, similar to incomplete γ-function

$$f(K_\gamma) = A \times K_\gamma^\alpha \times exp\ (-K_\gamma/\beta), \quad \langle K_\gamma \rangle = (\alpha + 1) \times \beta \tag{19}$$

For example, if $\alpha = 1.5$ and $\beta = 0.075$ average $< K_\gamma >$ has quite reasonable values equal to 0.188. However, the condition $E_h^\gamma > 4$ TeV makes $< K_\gamma >$ dependent on E_h (Figure 4a).

Therefore the more important parameter is not $\langle K_\gamma \rangle$ but K_{eff}

$$K_{eff} = \int\int K_\gamma f(K_\gamma) F(E_h) dE_h dK_\gamma \tag{20}$$

TABLE VI: Average values of parameters, P_A, and their dissipation, D_P, in simulated families.

	n_h	R_γ (cm)	R_γ^E	$E_\gamma R_\gamma$	d	q_n	q_E
P	2.7	2.8	2.4	24.	.59	.10	.10
D_P	2.4	1.5	1.6	15.	.16	.07	.11
P^{α}	2.5	2.7	2.3	24.	.60	.10	.10
D_P	2.4	1.4	1.5	14.	.16	.08	.10
He	3.3	3.2	2.9	30.	.63	.12	.20
D_{He}	2.8	1.6	1.7	17.	.16	.08	.11
CNO	4.3	4.0	3.6	34.	.69	.14	.15
D_{CNO}	3.2	1.7	1.9	17.	.13	.08	.10
SiMg	5.0	4.5	4.1	38.	.72	.16	.16
D_{SiMg}	4.0	1.8	2.0	19.	.13	.08	.11
Fe	6.3	4.8	4.4	40.	.74	.18	.19
D_{Fe}	4.7	1.9	2.1	18.	.13	.09	.11

Here $F(E_h)dE_h$ is the energy spectrum of hadrons in families. As calculations shown for simulated families $K_{eff} = 0.23$. This value is quite compatible with that offered in [29]. Distributions of K_γ obtained in [29] for Pamir chamber and our approximation of $f(K_\gamma)$ are given in Figure 4b. They are in a reasonable agreement. Knowing probability of hadron interaction, its energy and distribution of K_γ and using Monte-Carlo method one gets for each hadron answers to questions: whether hadron interact in the chamber? what energy it transfers into soft component $E_h^\gamma = (K_\gamma E_h)$? and whether it is registered, i.e. E_h^γ is more than $E_{thr} = 4$ TeV? Such algorithm was applied to simulated families to get hadron characteristics: n_h, q_n, q_E, etc. Average values of sensitive ($S > 0.5$) parameters of families, P_A, and their dispersions, D_P, for various primary nuclei(P^α - Protons with energy spectrum having "knee") are brought in Table VI.

TABLE VII: Expected values of families characteristics at various chemical compositions.

	n_h	R_γ	R_γ^E	$R_\gamma E_\gamma$	d	q_n	q_E
Normal	3.2	3.0	2.6	26.	.62	.11	.11
Heavy	3.6	3.3	2.9	29.	.64	.12	.12
Superheavy	4.2	3.7	3.3	32.	.66	.13	.14

Dependencies of n_h, R_γ and d on A are shown in Figures 5a and 5b. As above characteristics of families for all nuclei are calculated at integral energy spectrum index $\gamma = -1.7$. Data for families generated by protons having power spectrum with bend in point $E_0 = 3\times10^{15}$ eV are brought in the third and fourth lines. Up to the bend $\gamma = -1.7$, after $\gamma = -2.2$. TableVI shows that the "knee" of the spectrum insignificant influences on average characteristics of proton induced families.

One can calculate expected values of parameters for the given CC (Table VII) with the help of expression (18) and using Tables I, III and VI where various compositions, C_A, efficiency of family's generation, ϵ_A, and the average values of parameters, P_A, are given.

Comparison of Tables V and VII shows that characteristics of families at normal composition are in good agreement with the experimental data whereas predictions for heavy and the more so for superheavy compositions differ much from the observations. This subject is discussed in the next two subsections.

4. Comparison of the experimental data with the results of MC0 model.

Detailed comparison of the experimental data with the results of MC0 model is given in the following two subsections. In the first one χ^2 test is applied to the above mentioned sensitive parameters but before parameters uncorrelated between each others were found out. All of them show a much better agreement with the results corresponding to the normal chemical composition than that at the heavy compositions. In the next subsection not only sensitive but other main parameters of families are attracted to the analyze with the aim of study the possible systematic errors in the experiment. Here also good agreement with

calculations at the normal chemical composition is achieved.

4.1 Compatibility of the experimental data with the results of MC0 model.

Before making the final conclusions about chemical composition of PCR by comparison of experimental data (Table V) with predictions of MC0 model (Table VII) one has to find out which of the studied characteristics are not correlated. Otherwise traditional (for example, χ^2) and not traditional (neural net) approaches can incorrectly estimate a degree of agreement of experimental and simulated data. Among selected seven parameters sensitive to chemical composition (Table VI) there are 2 groups of strongly correlated characteristics. They are characteristics related to the energy of hadrons, n_h, q_n, q_E (for example see Figure 6a) and spatial characteristics of γ-quanta, $R_\gamma, R_\gamma^E, E_\gamma R_\gamma$ (Figure 6b). Stands to apart parameter d, which weekly correlate with both of the groups (Figure 6c). Parameters belonging to the different classes do not correlate also (Figure 6d). We have chosen three sensitive and not correlated parameters: n_h, R_γ, and d. Only they are used in the subsequent analysis. For comparisons of the experimental and simulated families the following quantities were calculated:

$$\chi_p^2 = [(P_{exp} - P_{mod})/\sigma P_{exp}]^2 \tag{21}$$

and sum for three not correlated parameters

$$\chi_3^2 = [[(n_{hexp} - n_{hmod})/\sigma n_{hexp}]^2 + [(R_{\gamma exp} - R_{\gamma mod})/\sigma R_{\gamma exp}]^2 + [(d_{exp} - d_{mod})/\sigma d_{exp}]^2] \ / \ 3 \tag{22}$$

Here P_{exp} and P_{mod} are an average value of some parameter but σP_{exp} is an error of P_{exp}. Instead of total error $(\sigma_{exp}^2 + \sigma_{mod}^2)$ only corresponding σ_{exp}^2 stands in (21) and (22) since statistical errors in calculations are much less than experimental uncertainties. The results are shown in Table VIII.

Each χ^2 should be near one if the experiment and calculations are in a good agreement, since the number of degrees of freedom for separate parameter is 1 and χ_3^2 is an appropriate

TABLE VIII: Values χ^2_p for various parameters and χ^2_3.

CC	χ^2_{nh}	$\chi^2_{R\gamma}$	χ^2_d	χ^2_3
Normal	0.11	3.4	0.95	1.5
Heavy	2.7	20.	0.24	7.7
Superheavy	13.	54.	7.2	25.

χ^2 with the 3 degrees of freedom divided on 3. This expectation is fulfilled only for the normal composition, but is not satisfied for the heavy and superheavy compositions. It is necessary to notice, that rather large values of $\chi^2_{R\gamma}$ =3.4 for the normal composition can indicate on the presence of some systematic errors. This problem will be analyzed in the next subsection. The dependence of χ^2_3 on $< lnA >$ is shown in Figure 7. Dotted line corresponds to χ^2_3 =4. Confidence level at χ^2 =4 is less than 1%. Figure 7 shows that all compositions with $< lnA >$ more than 2.5 are above the line and therefore can be excluded with confidence level more than 99%.

4.2 Consents of MC0 model with the experimental data. Systematic errors.

It was shown in the previous section that MC0 model with normal chemical composition of PCR is in a reasonable agreement with experimental data. Nevertheless two circumstances cause doubt. Firstly, experimental average radius of families $R_\gamma = 2.8 \pm 0.1$ appears to be less than calculated radiuses at any chemical compositions R_γ = 3.0 - 3.7 (Table V and VII). This is the cause of a little bit large values $\chi^2_{R\gamma}$=3.4 and accordingly χ^2_3=1.5 for the normal CC (Table VIII). For heavy compositions these quantities are much more. Secondly, experimental average values of $n_\gamma = 21 \pm 2$ is less than calculated $n_\gamma = 24 - 26$ at any chemical composition. Till now n_γ was not interesting as it does not depend on atomic number of incident nuclei (see Figure 3b). There is a suspicion that R_γ and n_γ are subject of some systematic experimental errors and it is desirable to find their common origin. In this subsection we want to carry out the more complete analysis of the consent of MC0 model with experimental data considering possible systematic errors at measurement

TABLE IX: Values of parameters, P, and their χ^2_P.

Exp and CC	Param.	n_h	R_γ	d	q_n	$E_\gamma R_\gamma$	n_γ	E_γ
Exp	P	3.1	2.8	.63	.11	27.	21.	12.1
	σ_P	0.3	.01	.01	.01	2.	2.	0.5
Normal	P	3.2	3.0	.62	.11	26.	24.	11.1
	χ^2_P	0.11	3.4	.95	.06	1.3	13.	3.1
Heavy	P	3.6	3.3	.64	.12	29.	25.	10.8
	χ^2_P	2.71	20.	.24	1.5	0.86	20.	7.0
Superheavy	P	4.2	3.7	.66	.13	32.	26.	10.5
	χ^2_P	13.	54.	7.2	9.5	5.2	25.	12.4

of parameters. Values of the most important parameters characterizing γ-hadron families measured in the our experiment and predicted by MC0 model for various CC together with χ^2_P are brought in Table IX. As already was noted the most serious deviation of model from experimental data is displayed in parameters R_γ and n_γ. For heavy composition this disagreement is even stronger than at the normal CC. The common reason of all large deviations can be systematic errors in energy determination, E_γ, by measurement of spot's darkness, D, on a X-ray film. The algorithm of transition from D to E_γ is rather complex. Besides theoretical connection between energy of γ-quantum and the number of electrons in a circle of certain radius under given thickness of lead where a film is located (transition from E_γ to n_e) it includes the property of the film ($n_e \to D$ curve, saturation of D at large n_e etc), condition of the exposition of the film (its background, gap between the film and lead plate) and so on. All these effects mostly are accounted and controlled. However, it is not excluded that some of discrepancy can nevertheless be left. Group effects in families are added to these problems - partial overlapping of spots and even their aggregation (the last effect we took into account at processing of simulated families). To study an influence of energy measurement errors on family's characteristics we have added to simulation of events

modeling of distortion by replacing E_{true} to E_{meas}.

For this we used some distortion functions, $f(E)$:

$$f(E_{true}) = E_{meas}/E_{true} \tag{23}$$

Two distortion functions were tested :

$$f_1(E_{true}) = 10/E_{true} \times (E_{true}/10)^{\alpha} \tag{24}$$

with $\alpha > 1$ ($\alpha < 1$) up to 10 TeV and $\alpha < 1$ ($\alpha > 1$) after 10 TeV to provide underestimation (overestimation) of true energy

and

$$f_2(E_{true}) = 70/E_{true} \times (E_{true}/70)^{\beta} \tag{25}$$

with $\beta < 1$ in the whole interval of E_{true}. Parameters α and β were varied. Typical examples of distortion functions are shown in Figure 8. At the particular chose of α, function $f_1(E)$ reflects underestimation of energy up to and after E_{true}=10 TeV with different dependence of E_{meas} on E_{true}. Opposite to $f_1(E)$, $f_2(E)$ overestimates true energy up to 70 TeV and then underestimates it. $f_2(E)$ was taken from work[30]. An attempt of modeling of passage of γ-quanta through the lead plates of the chamber and then its fixing on a film with the accounts of peculiarities mentioned above was carried out there. Various values of α were set in calculations to ensure $10\%, 20\%, 50\%$, (-20% and -40%) underestimation (overestimation) of energy near measured threshold 4 TeV and $-5\%, -10\%, -20\%$ underestimation of energy at true energy 100TeV. Dependencies of χ^2_P for the normal chemical composition on a degree of energy underestimation or overestimation in Figure 9a ,9b. The Figures show that all χ^2_P have quite admissible values already at 10% of underestimation of energy (E_{true} = 4.4 TeV instead E_{meas}= 4 TeV) and no systematic errors at 100TeV ($E_{meas} = E_{true}$ at E_{true} >100 TeV). It doesn't means absence of systematic errors at large energy E_{true} >100 TeV. Simply it appears that values χ^2_P weekly depend on an underestimation of energy at E_{true} >100 TeV (Figure 9b). As the 10% systematic error is quite

TABLE X: χ^2_P values for normal and heavy chemical compositions at 10% and 20% underestimation of energy near the threshold.

CC	E_{true}	n_h	R_γ	d	q_n	$E_\gamma R_\gamma$	n_γ	E_γ	χ^2_3
Normal	4.4	0.09	1.85	.11	.02	0.11	3.4	1.37	0.70
Heavy	4.8	0.63	7.39	2.65	1.84	1.88	4.63	2.15	3.60

possible we conclude once more that MC0 model at the normal chemical composition is in a very good agreement with the experimental data. Situation at heavy and the more so at superheavy compositions is different. In the previous section it was shown that they contradict to the experiment. Figure 9c, similar to 9a, for heavy composition shows that no one distortion function can improve the consent of MC0 model with the experiment at heavy composition. χ^2_P for normal and heavy chemical compositions at the most favorable distortion functions for each of them are given in Table X. We should note that in the case of superheavy composition χ^2_P values are so large that this composition is out of consideration.

Finally let us discuss the predicted intensity of families at used distortion functions. Since after introduction of distortion functions the number of events, satisfying the selection criteria of families, decreases, diminished also expected intensity of families. For the normal composition at $E_{true} = 4.4$ TeV the intensity become equal to $I_{fam} = (0.58 \pm 0.18)$ m^{-2} year^{-1} srt^{-1} . For the heavy composition at $E_{true} = 4.8$ TeV $I_{fam} = (0.25 \pm 0.08)$ m^{-2} year^{-1} srt^{-1}. Let us remind that experimental intensity is (0.43 ± 0.12) m^{-2} year^{-1} srt^{-1}. From the given figures it is apparent that after corrections for possible systematic errors the conclusions made in section 2 concerning chemical compositions based on intensity of families strengthen.

We have used a number of procedures simulating process of γ-quanta and hadrons registration in X-ray chamber. These are: a procedure of aggregation (unification near-by spots); an ascription to each hadron a factor of energy transfer into soft component, K_γ, distributed according to incomplete γ-function; possible underestimation of energy threshold

of γ-quanta and hadrons, E_{thr}; an account for systematic underestimation of energy of the most energetic γ-quanta (replacement in simulations E_{true} to E_{meas}). This can appear to be not correct and artificial. Actually, as any complex installation, X-ray emulsion chamber brings in certain distortions in NEC falling on it. As a result instead of true parameters, P_{true}, one has to do with their measured values, P_{meas}. To have an opportunity to compare parameters measured in experiment with that of simulated, it is necessary to model processes occurring in X-ray emulsion chamber. In Pamir collaboration the routine, carrying out this problem is named the code of "passages through the chamber"[30]. This code is rather complex and is an analogue of routine JEANT [31], used at accelerators for imitation of distortions, connected with this or that installation: ATLAS, CMS and others[32, 33]. In the present work "the program of passage through the chamber" was divided on stapes (aggregation, $K_\gamma, E_{true} \to E_{meas}$) to look after influence of each of the effects separately. By such approach we have resulted in the conclusions about a role of each type of distortions in determination of measured parameters of families.

5. Selections of families generated by iron nuclei.

The attempt of selections of families similar to that induced iron(Fe)nuclei by means of image recognition methods were done in the several papers. All of them claim that compositions enriched with heavy components are in contradiction to experimental results. Only compositions near to the normal can satisfy them. The description of the method and short review of the mentioned works are given in the subsection 5.1. In the next subsection our original investigations are brought. The most encouraging is the result of reconstruction the fraction of Fe-like families inputted into calculations by the method, which is proposed. The main conclusion is again only results at the normal composition are consistent with the experiment.

5.1 Selections of families generated by iron nuclei. A short review.

The attempt to determine a fraction of iron nuclei in PCR on a database of X-ray-emulsion chamber was undertaken in work [27, 34, 35] for the first time. Almost simultaneously by

two groups of authors it was offered to apply to family multidimensional analysis of an image recognition. The sense of it is that using a difference in distributions of some parameter of families generated by iron and proton (see Fig. 3a) one defines a limiting value for the given parameter, P_{lim}. Event with $P_{fam} \geq P_{lim}$, is considered as a family similar to one generated by iron. Such an event is attributed to group of families "Fe". Otherwise if $P_{fam} < P_{lim}$, then family is added to group "P". A fraction of families, f', " similar to iron " is thus defined. Multidimensional method of an image recognition means that the limiting values are defined for several parameters P^1_{lim}, P^2_{lim}, P^3_{lim} .... Families which simultaneously satisfy the requirements:

$$P^1 \geq P^1_{lim}, \qquad P^2 \geq P^2_{lim} ...$$

are attributed to group "Fe".

Fraction of families induced by nuclei A and satisfying the limiting conditions (Fe-like produced events) are designated R_A.

Two types of errors in the image recognition method. The error of the first type is to attribute families from proton to "Fe" group (R_P) and the error of the second type is not to "recognise" iron family and not to added it to "Fe" group, $(1 - R_{Fe})$. The quality of selection is defined by values of these two errors. As more sensitive are the parameters to atomic number, the stronger differ distributions of parameters for P and Fe families. As a consequence cleaner and more complete is the selection as both errors are small. The error of the first type includes all families from other primary nuclei (except Fe) falsely attributed to the "Fe" group.

Quasi-scaling models were used for determination of limiting values of parameters $P_{lim}{}^i$ in three mentioned works. Training sets of families generated by P and Fe were simulated and distributions, similar to that shown in Figure 3, were obtained. These distributions allowed determination of the boundary quantities $P_{lim}{}^i$. It was found [27, 34] that it is impossible to use simultaneously more than two parameters because of limited statistics of families. Therefore either $E_\gamma R_\gamma$ and asymmetry parameter of family, b, or $E_\gamma R_\gamma$ and n_γ were

used in [34]. Another parameter of asymmetry, α, and parameter d, used in the previous sections, or their combination with R_γ were involved in [27]. Parameters d, α and $1/R_\gamma^E$ in different combinations were analyzed in [35].

The fraction of families attributed to group "Fe", f', is equal to

$$f' = f \times R_{Fe} + (1 - f) \times R_P \tag{26}$$

where f is the real fraction of families generated by iron. From (26)

$$f = (f' - R_P)/(R_{Fe} + R_P) \tag{27}$$

Authors of the all three works ([27, 34, 35]) applying the described method to families of Pamir Collaboration have found that the fraction of families generated by iron does not exceed 2-3 %, i.e. that the compositions of PCR with domination of iron contradict to the experiment.

The method of selection families generated by iron was essentially improved in work [6], where experimental data of Pamir-Chacaltaya Collaborations were used. In contrast to us (see conditions (2)) in papers based on Joint Pamir-Chacaltaya experiment a group of γ-quanta and hadrons with $\Sigma E_\gamma + \Sigma E_h^\gamma$ >100 TeV at E_γ and $E_h^\gamma > 4$ TeV was considered as a family [6]. For recognition of an image of a family produced by iron author of [6!!] used a neural net method, with the help of which multi-dimensional analysis is reduced to one-dimensional. 15 parameters describing a family were used in [6]: n_γ, n_h, ΣE_γ, ΣE_h and so on. With the help of neural net the set of them was reduced to one, y_p, and condition which attributes a family to the "Fe" group was y_p >0.5. The quality of selection making by this way has appeared to be rather high: $R_P \approx (1 - R_{Fe}) \approx 15\%$.

Also the next step on the way of CC study was made in [6]: not only families produced by P and Fe but also generated by other nuclei (He and CNO, SiMg groups) were examined there. It means that these nuclei also contribute to group "Fe". Following our consideration in this case(24) should be transformed to:

$$f' = \Sigma(f_A \times R_A) \tag{28}$$

and accordingly

$$f = (f' - \Sigma'(f_A \times R_A))/R_{Fe} \tag{29}$$

Here f_A is a fraction of families generated by nuclei A, R_A - their fraction faulty attributed to group "Fe" (except R_{Fe}, R_{Fe} is true portion), f' - the part of families satisfying the limiting condition. In $\Sigma(f_A \times R_A)$ contributions of all nuclei are summarized, in $\Sigma'(f_A \times R_A)$ iron families are not included. Let us underline once more that we designate true value of Fe induced families as f_{Fe} and estimated by (28) as f. The training sets define R_A and the given chemical composition of PCR determines f_A (see (1) and Table II.

The conclusion of [6] is the same as in previous works [34, 27, 35]: the heavy composition of PCR is excluded by experimental data concerning γ-hadron families.

For the sake of completeness of the review refer to work [8]. In this work rather complex parameters, reflecting structural properties of families, and intensity of "structural" families are used. The conclusion in [8] is opposite to the above-stated. Authors affirm that the superheavy composition of PCR is necessary for description of considered properties. As one of the critical remarks to [8] let us note that authors of [8] did not show that the model they used describes the more simple characteristics of families at the superheavy composition.

5.2 Selections of families generated by iron nuclei. Original consideration.

We have used methods similar to multi-dimensional [27, 34] and one-dimensional [6] approaches as a following step of chemical composition researches. Before starting CC analysis we have found parameters n_γ, R_γ, and d sensitive to A and are not correlated between each other (section 3). In contrast to [6, 27, 34] we used only them. The parameters are analyzed in their reduced form:

$$X_P = (P - P_p)/\delta P_p \tag{30}$$

Here P is a value of some parameter in a given family either experimental or simulated, P_P - average values of the same parameter in families induced by protons, δP_P - disipation of this parameter in proton families.

In reduced form of variables all distributions are dimensionless and for families generated by protons are dispersed around average values $X_P = 0$. At multidimensional analysis simultaneously three conditions were used to attribute a family to "Fe" group:

$$X_{n_h} > X_{n_h\ lim}, \quad X_{R_\gamma} > X_{R_\gamma\ lim}, \quad X_d > X_{d\ lim} \tag{31}$$

For one-dimensional analysis a new parameter X_3, was introduced:

$$X_3 = (X_{n_h} + X_{R_\gamma} + X_d)/3 \tag{32}$$

For this parameter a value $X_{3\ lim}$ was also found and the family was attributed to group "Fe" if its

$$X_3 > X_{3\ lim} \tag{33}$$

Limiting conditions P_{lim} were determined with the help of integral distributions of X_P for families induced by P and Fe using training sets of simulations. Integral distributions at once show what fraction of proton families (R_P) at the given P_{lim} will be by mistake attributed to "Fe" group and what fraction of iron families will not recognized as Fe-like, (1-R_{Fe}). An example of such distribution is given in Figure 10. The arrows in Figure 10 indicate limiting values of X_3. One of them corresponds to about equal errors $R_P = (1 - R_{Fe}) \approx 20\%$, while the other - to $R_P = 5\%$ and $(1 - R_{Fe}) \approx 40\%$.

It is apparent that both errors R_P and $1 - R_{Fe}$ depend on chosen limits $X_{n_h\ lim}$, $X_{R_\gamma\ lim}$, $X_{d\ lim}$, and $X_{3\ lim}$. We investigated two sets of limiting parameters. First, at which $R_P = 5\%$, i.e. only 5% of proton families are falsely attributed to "Fe" group, and second, such that the errors of the first and second types are approximately equal $R_P \approx (1 - R_{Fe})$. True values of fraction iron induced families, f_{Fe}(see Table II), and expected fraction of families, selected to group "Fe", f', for different chemical compositions are brought in Table XI at

TABLE XI: True fraction of Fe families, f_{Fe}, and expected fraction of Fe-like families,$f^{'}$,at various chemical compositions

.

	CC	f_{Fe}%, true	$f^{'}$%, one-dim.	$f^{'}$%, multi-dim.
$R_P = 5\%$	Normal	2.8	13.	11.
	Heavy	16.4	21.	19.
	Superheavy	31.	30.	28.
	Exp.		12.±3.	11.±3.
$R_P = 20\%$	Normal	2.8	26.	27.
	Heavy	16.4	35.	37.
	Superheavy	31.	47.	47.
	Exp.		29.±4.	25.±4.

two sets of limiting parameters $X_{P\ lim}$. Let us remind that f_{Fe} is fully determined by the given CC while $f^{'}$ is the result of processing of simulated data for set of limiting parameters.

Table XI is composed using training sets for various nuclei P, He, CNO, SiMg and Fe. R_A was determined for each nucleus and then the sum $f^{'} = \Sigma(f_A \times R_A)$ was found. We should like to pay attention to the fact that for normal composition the true iron families figural spiking is lost among families selected in "Fe" group. At the normal composition the true Fe fraction $f_{Fe} = 2.8\%$ while Fe-like proton $f^{'}$ varies from 11%-to 27% depending on R_P.

To check efficiency of the used method to determine a part of Fe induced families we have investigated how it reproduces f_{Fe} at various chemical compositions. The results (f) are given in Table XII for one particular selection (multi-dimensional selection, $R_P = 20\%$). Results of the other three selections (multi-dimensional $R_P = 5\%$, one-dimensional at $R_P =$ 20% and 5%) are identical.

In Table XII rows correspond to simulated compositions, columns to compositions by means of which corrections were done using (29) . For comparison f with the true values of

TABLE XII: Fractions of iron induced families, f , in chemical composition of families, calculated by (29). Multi-dimensional selection, $R_P = 20\%$

.

	P	Normal	Heavy	Superheavy	Fe	f_{Fe},%
P	**0.2±2.5**	-4.3±	-2.6±	-1.2±	27.±2.5	0
Normal	8.7±1.7	**4.2±1.7**	5.9±1.7	7.3±1.7	36.±1.7	2.8
Heavy	21.±2.4	16.±2.4	**18.±2.4**	19.±2.4	48.±	16.4
Superheavy	35.±2.7	30.±2.7	32.±2.7	**34.±2.7**	62.±2.7	31.
Fe	79.±6.4	75.±6.4	76.±6.4	78.±6.4	**106.±6.4**	100
Exp.	5.9±5.0	**1.4±5.0**	3.1±5.0	4.5±5.0	33.±5.	**?**

f_{Fe} the letter for each simulated compositions are given in the last column of the Table.

Table XII demonstrates rather encouraging result. Independently to the composition used for corrections (for exception of pure Fe), the fractions f are close to corresponding true value. As it is expected the best agreement f with true f_{Fe} is obtained if the composition for corrections is close to the "real". The corresponding figures are underlined in Table XII. From the above the following procedure of processing of experimental data is suggested. After determining an experimental value $f^{'}$ corrections should be done for various CC, for example for five compositions testing in Table XII. Then receiving preliminary result (five values for f) one takes that at which chemical composition determining corrections is closest to obtained f. This is shown in the last row of Table XII. The final value of found fraction of Fe induced families is underlined.

The total analysis of our experimental data was as follows. Four values of fractions of families similar to iron, $f^{'}$, were found corresponding to two type of the methods (multi-dimensional and one-dimensional) and two sets of limiting parameters for $R_p = 5\%$ and $R_p = 20\%$. They are brought in the last row of Table XI. Values f were reproduced

by the help (29). Quantities f are given in the last row of Table XII corresponding to various correction compositions. Table XII shows, that only normal composition gives self consistent values f. In this case true values $f_{Fe} = 2.8\%$ and set of experimental quantities of f fluctuates from 1.4% to 4.5%. In the case of the heavy composition the experimental fraction $f = 3.1\%$ contradicts to true value $f_{Fe} = 16.4\%$. Even more disagreement shows the superheavy composition: true $f_{Fe} = 31\%$ while obtained f is equal to 4,5%.

As it was specified above we have tested four selections criteria of Fe-like families. Table XII is given for one of them. The results of all other selections are identical: events, generated by iron nuclei, compose about (2 - 3)%. This is in agreement with the normal composition and sharply contradicts to compositions enriched by iron.

6. Conclusion

The purpose of the present work was an investigation of Chemical Composition of Primary Cosmic Rays with energy around 10^{16} eV close to the "knee" of energy spectrum of PCR. In this region of energy information about CC of PCR can be obtained only by an indirect way on the base of study of extensive air showers or families of γ-quanta and hadrons registered by X-ray emulsion chambers.

In the present work the data of Pamir and Pamir-Chacaltaya Collaborations concerning families were used. The analysis of a material was made by means of comparison of the experimental families with that simulated by quasi-scaling model MC0 [5].

First of all it was shown that MC0 at normal CC (close to composition at 10^{14}eV, about 40% P and 20% Fe) predicts intensity of families in complete agreement with experimental observations (section 2). Thus long-term dispute, heavy chemical composition or strong scaling violation in the fragmentation region was solved.

Further it was shown that not only intensity, but also all main characteristic of families (they are about 15) are well described by MC0 at normal chemical composition (section 3).

Characteristics of families sensitive to atomic number of an incident nucleus were found out on the base of simulated events generated by primary protons and iron. Among them 3

parameters not correlating with each others were chosen. They are number of hadrons n_h, radius of a family R_γ and parameter d, describing electromagnetic structure of an event. It has appeared that their average values in experiment are close to the same in artificial families at the normal composition of PCR and are in disagreement with the heavy (15% P and 58% Fe) and, especially, with the superheavy (7% P and 70% Fe) compositions. χ^2_3 was calculated for the three above mentioned parameters. In the case of the normal CC it is equal to 1.9, for two iron enriched CC χ^2_3= 7.7 and 25. correspondingly (subsection4.1).

Despite of the rather good agreement of experiment and calculations at the normal composition two basic characteristics of families n_γ and R_γ have rather significant deviations from expected values: $\chi^2_{n_\gamma}$=13. and $\chi^2_{R_\gamma}$= 3.4. The investigations have shown that if one admits 10% underestimation of energy near to registration threshold of γ-quanta (about 4 TeV) and introduces the appropriate distortion function into simulated families, then corresponding χ^2 become equal to $\chi^2_{n_\gamma}$= 3.4 and $\chi^2_{R_\gamma}$=1.85 (subsection4.2). At 20% underestimation of energy χ^2 for all characteristics of families are close to 1. On the other hand any underestimation or overestimation of energy do not bring to an agreement between experimental average characteristics of families to those simulated at heavy and superheavy compositions.

Another attempt to investigate chemical composition was based on the selection of families similar to that generated by iron. Such method was already applied to experimental data of Pamir [27, 34, 35] and Pamir-Chacaltaya Collaborations [6].In all four investigations fraction of Fe-generation γ-hadron families was small and equal 2-3% . Thus it appear that the heavy compositions contradict to the fraction of families from Fe in the experimental data.

In this article we continued elaboration of an application of image recognition methods to CC research by means of families (sections 5). Limiting values ($X_{P\ lim}$) for the three above mentioned sensitive parameters (P) in their reduced form X_P were determined (section 5). Families with $X_P > X_{P\ lim}$ were attributed to "Fe" group. A united parameter $X_3 = (X_{n_\gamma} + X_{R_\gamma} + X_d)/3$ with its $X_{3\ lim}$ was also used. Ability of the method was investigated by the help of simulated families. Sets of families generated by pure protons and irons as

well as by the normal, heavy and superheavy chemical compositions were analyzed. Families "similar" to iron were selected for all these sets. The fractions of Fe-like families and the restored ((29)) parts of "true" Fe families were estimated. For each set of simulations the found "true" fraction of Fe-families were in coincidence with the fraction of Fe families in the given chemical composition.

The method of selection of Fe-like families was applied to experimental events. A fraction of families similar to that induced by iron was found. It appeared to be close to the appropriate fraction at the normal composition. After corrections by means of (29) the part of families from iron in the experimental set constitutes (2 - 3)%. Such value is in complete agreement with the normal CC and in sharp contradiction to the iron enriched compositions.

Thus the basic conclusions of the given work are:

MC0 model at the normal chemical composition completely agrees with the experimental data of γ-hadron families;

The chemical composition of Primary Cosmic Ray in the energy region near to 10^{16} eV just above the "knee" of its energy spectrum is close to the chemical composition at energy around 10^{14} eV;

The models of nuclear electromagnetic cascade in the Atmosphere with chemical compositions enriched by heavy elements contradict to the experimental data on families. They predict too low intensity of families, incorrect values of the characteristics of families and too large fraction of families generated by iron.

One more conclusion very important for the particle physics follows from the present work. All the quasi-scaling models [6, 12, 14, 15, 22, 23, 24], except MC0, give 2-3 times larger intensity of families than the observed one. It means that in these models hadron absorption mean free part is too large to provide proper intensity of families. Smaller mean free part in MC0 is due to large an inelasticity coefficient than in the other models. The better agreement of average characteristics of families in MC0 than in other models [22, 23, 24] is also the result of stronger absorption of hadrons. Therefore large an inelasticity coefficient is necessary feature of inelastic interactions at superhigh energies.

ACKNOWLEDGMENTS

The authors express their gratitude to all participants of Pamir Collaboration for long and fruitful joint work, R.Mukhamedshin for granting an opportunity to use the code MC0 developed by him and also M.Tamada for making available the data bank of Pamir-Chacaltaya Collaboration. Very useful were discussions with Dr.'s R.Mukhamedshin and M.Tamada.

REFERENCES

† Electronic address: ninarich@hepi.iph.edu.ge

[1] Watson A.A.//Proc. 25th ICRC V.8. P.257,(1997);
JACEE Collaboration //Proc. 24th ICRC OG 6.2.8, OG 6.1.14,(1995).

[2] JACEE Collabororation//Proc. 25th ICRC V.4. P.1,(1997).

[3] RUNJOB experiment // Proc. 25th ICRC V.4. P.133, 141, (1997).

[4] Nicolsky S.I.// Pros.3rd Int. Sym. on Cosmic Ray and Particl Physics 1984 P.507.

[5] Fedorova G.F.and Mukhamedshin R.A.// Bull Soc. Sci. Lettr. Lodz Ser. Rech. Def V.XVI. P.137,(1994).

[6] Tamada M.// J. Phys. G: Nucl. Phys. V.23. P.497, (1997) .

[7] Ren J.R.et al.// Phys. Rev. V.D38 P.1404, (1988) .

[8] Shibata M.// Phys. Rev. V. D24. P.1847, (1981) .

[9] Shibata T.// Proc. 24th ICRC V.8. P.10, (1995) ;
Stanev T, Bierman P L, Gaisser T K //98 astro-ph/9303006.

[10] Pamir Coll. //Proc. 20th ICRC V.7. P.385, (1997).

[11] Wrotniak J.A.// Zesz. nauk. Uh. V.7. P.148, (1977) .

[12] Dunaevsky A.M. et al.//Proc. 16th ICRC V.7. P.337, (1977);
Dunaevsky A.M.and Karpova S.A.// Bulletin de societe des sciences et des lettres de Lodz V.XVI. P.23,(1994).

[13] Fomin Yu.A.and Khricstiansen G.B.// Proc. 14th ICRC V.7. P.2574, (1975).

[14] Azimov S.A. Mullajanov E.J.and Yuldashbaev T.S.// Proc.18th ICRC V.5. P.462, (1983) .

[15] Knapp J. and Heck D. // KfK 5196B (1993).

[16] Krys A., Tomaszevski A. and Wrotniak J.A. // Proc. 16th ICRC V.7. P.188, (1979).

[17] Krys A., Tomaszevski A.and Wrotniak J.A.// Zesz. Nauk. UL V.32. P.5, (1980).

[18] Roinishvili N.N.// J. Phys. G: Part.Phys.(20), P.215, (1995).

[19] Pamir Collaboration, Mt.Fuji Collaboration and the Chacaltaya Collaboration // Nucl.

Phys. B391 P.1, (1981).

[20] Krys A. and Wrotniak J. A. et al. // Proc. 17th Intern. Cos. Ray Conf. V.5. P.315, (1981).

[21] Dunaevsky A.M. et al.// Proc. 5th Symp. Very High Energy Cosmic Ray Interaction P.143, (1988).

[22] Biolobrzeska H. et al. // Proc. 25th ICRC V.6 P.265, (1997).

[23] Bielawska H et al// Proc.25th ICRC V.6. P.269, (1997).

[24] Bielawska H et al// Proc.25th ICRC V.6. P.273, (1997).

[25] Pamir Collaboration // Proc. 21th ICRC HE-2, 4-22, (1990).

[26] Michalak W.// Zesz. Nauk. UL V.60. P.137, (1980).

[27] Asimov S A et el// Proc. 20th ICRC V.5. P.304, (1987).

[28] Bielawska H. and TomaszevskiA. // UL Pamir Collaboration Workshop P.38,(1980).

[29] Malinowski A et al // UL Pamir Collaboration Workshop P.49, (1980).

[30] Dunaevsky A.M.et al.// Proc. 5th Intr. Symp. VH Energy CRI P.93, (1988).

[31] CERN Program Library Long Writeup W5013 (1997).

[32] ATLAS Letterof Intent// CERN/LHCC/92-4 LHCC/I2, (1992).

[33] CMS Letter ofIntent // CERN/LHCC 92-3 LHCC/I1, (1992).

[34] Chilingarian A. et al.//Proc. 18th ICRC v.5, p.252, p 487,(1983); 19th ICRC v 6, p.392 (1985); 20th ICRC v.5, p.312, v.1,p.390 (1987).

[35] Yuldashdaev T.et al.//proc. 25th ICRC , v.4, p.89 (1997).

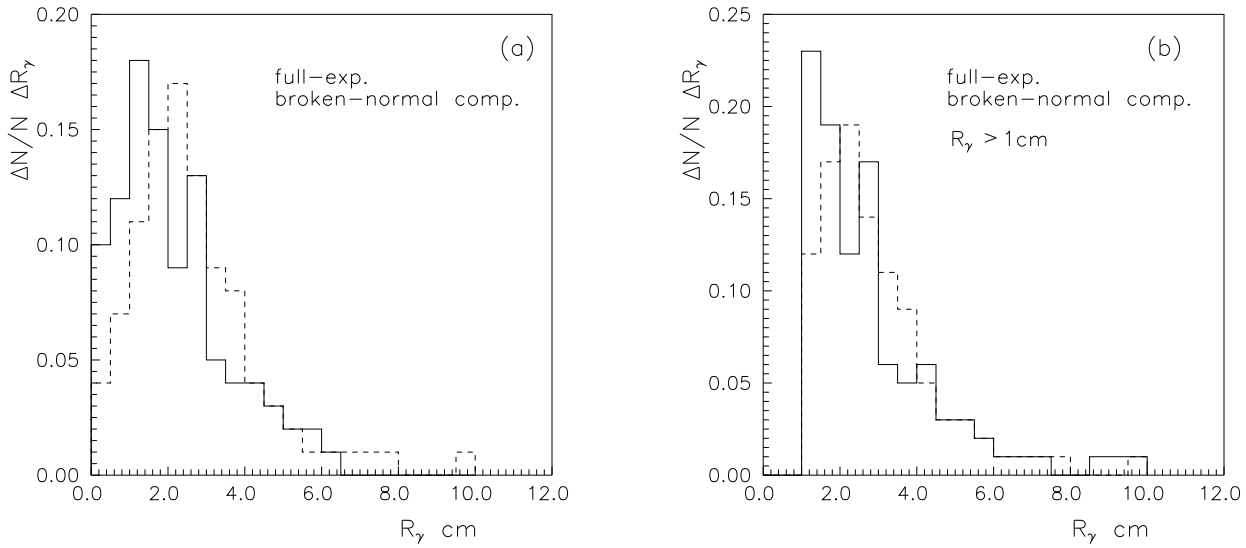

FIG. 1: R_γ - distributions. Continues line - experiment, dashed - normal CC. a) all families, b) families with R_γ >1cm.

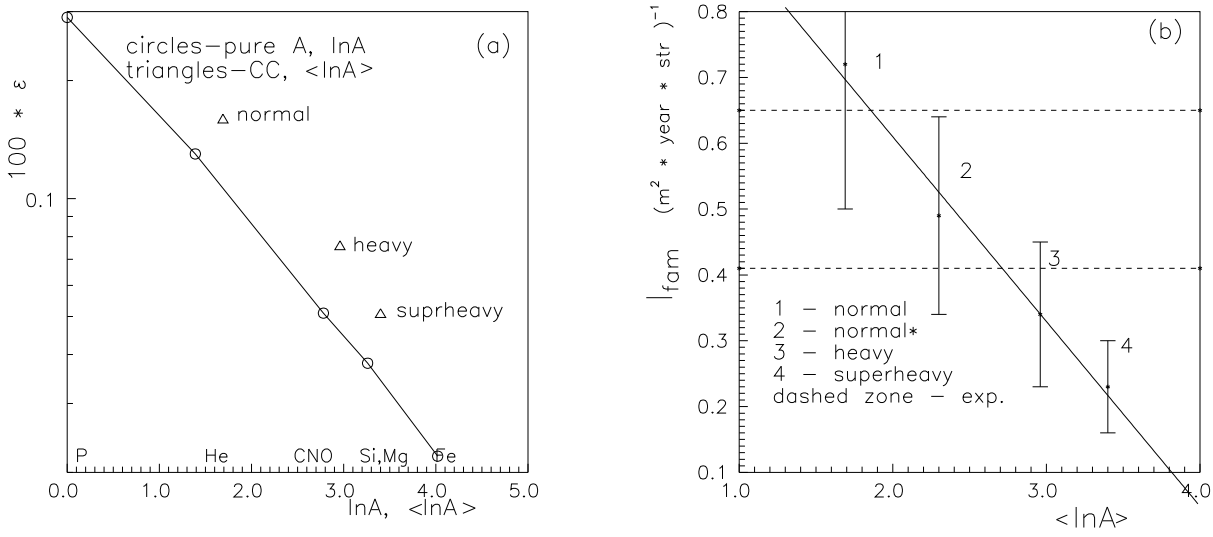

FIG. 2: a) Families production efficiency as function of $\ln A$. o - pure nuclei, Δ - different CC. b) Intensity of γ-families at different CC.

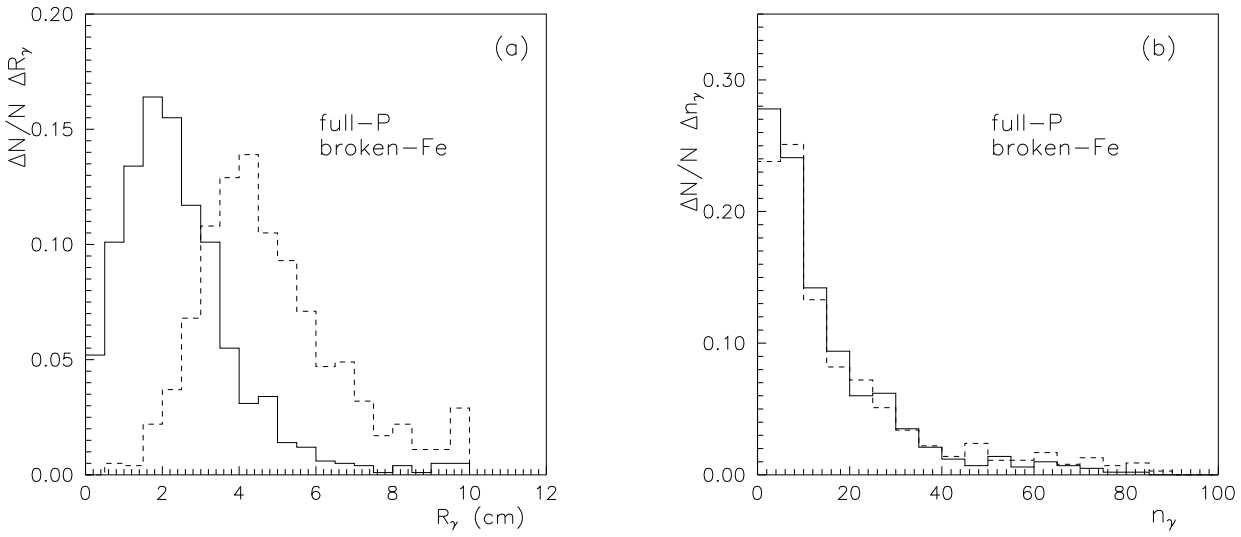

FIG. 3: Distributions of R_γ (a) and n_γ (b) for families generated by protons (continues line) and iron (dashed line).

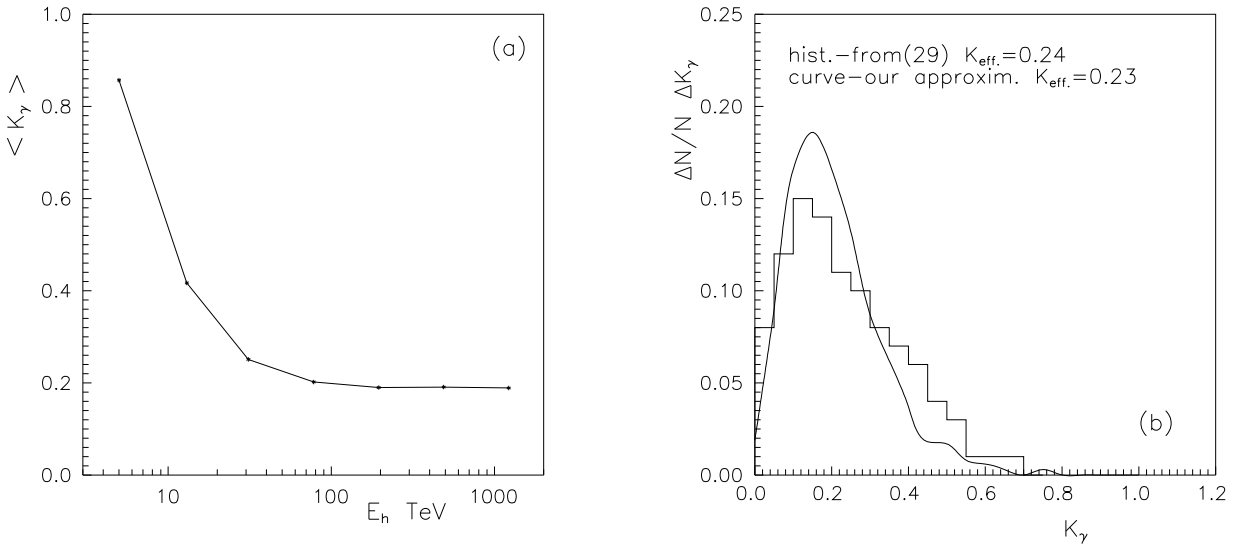

FIG. 4: a) Dependence of $\langle K_\gamma \rangle$ on E_h. b) K_{eff} distribution. Histogram is taken from [29], curve is used in this work.

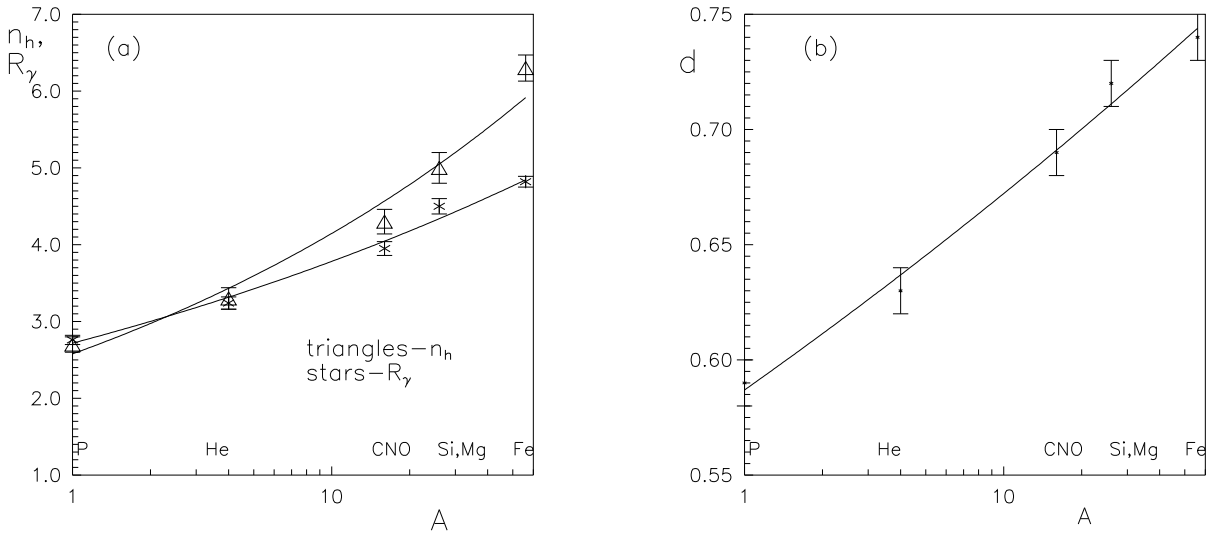

FIG. 5: a)n_h and R_γ dependencies on A. b) dependence of d on A.

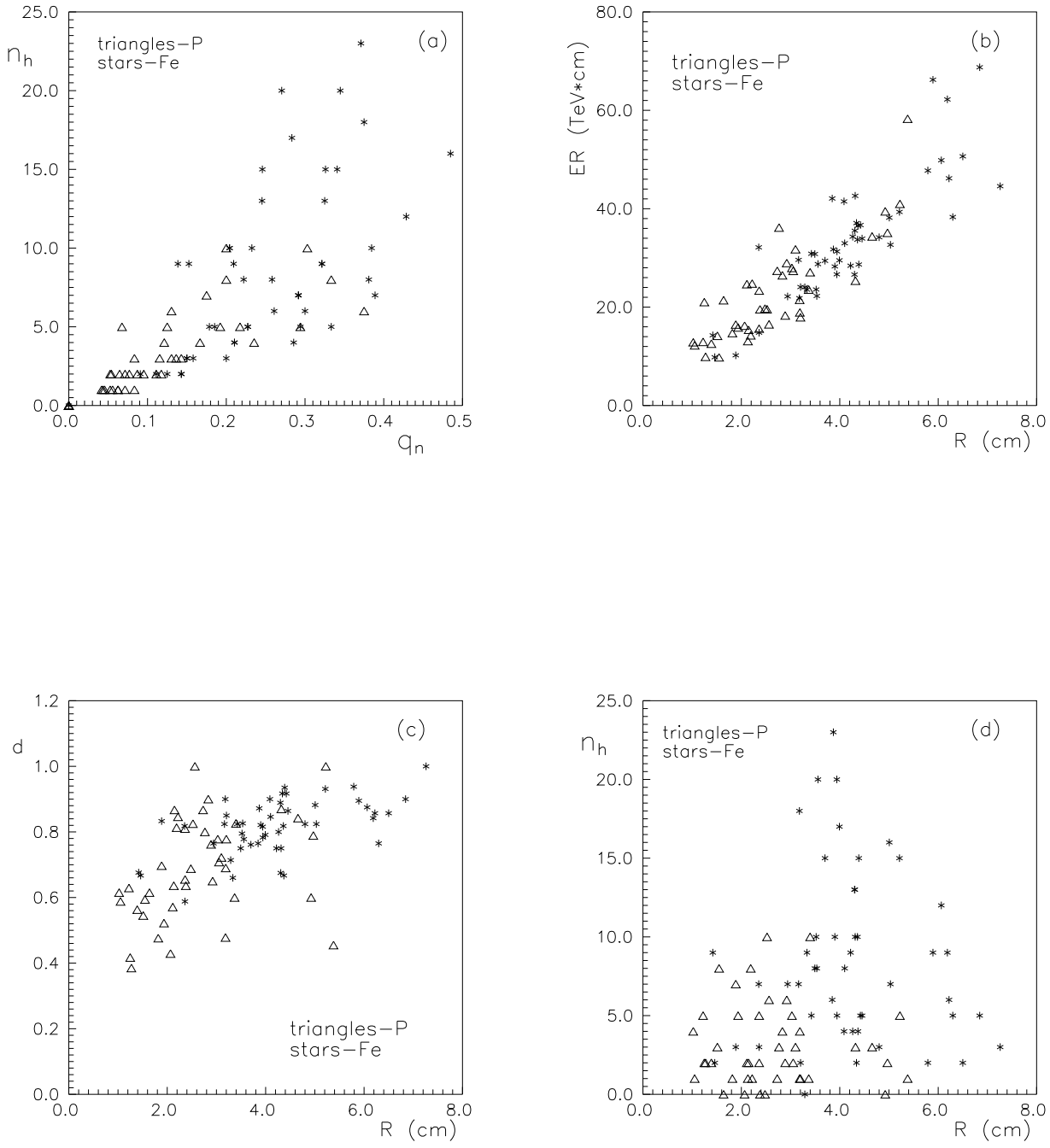

FIG. 6: Correlation: a)between n_h and q_h, k=0.60±0.02; b)between R_γ and ER_γ, k=0.88±0.01; c) between d and R_γ, k=0.34±0.03; d) between n_h and R_γ, k=0.00±0.04.

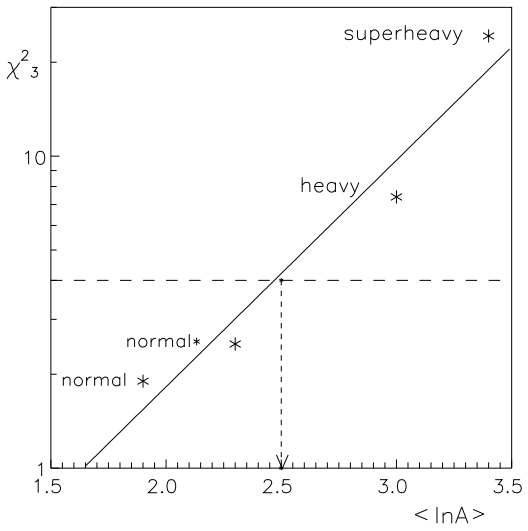

FIG. 7: Dependence of χ^2_3 on $\langle \ln A \rangle$.

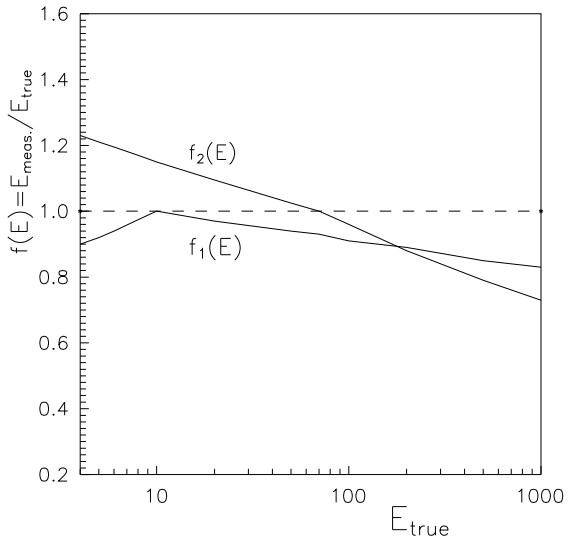

FIG. 8: Two types of distortion functions.

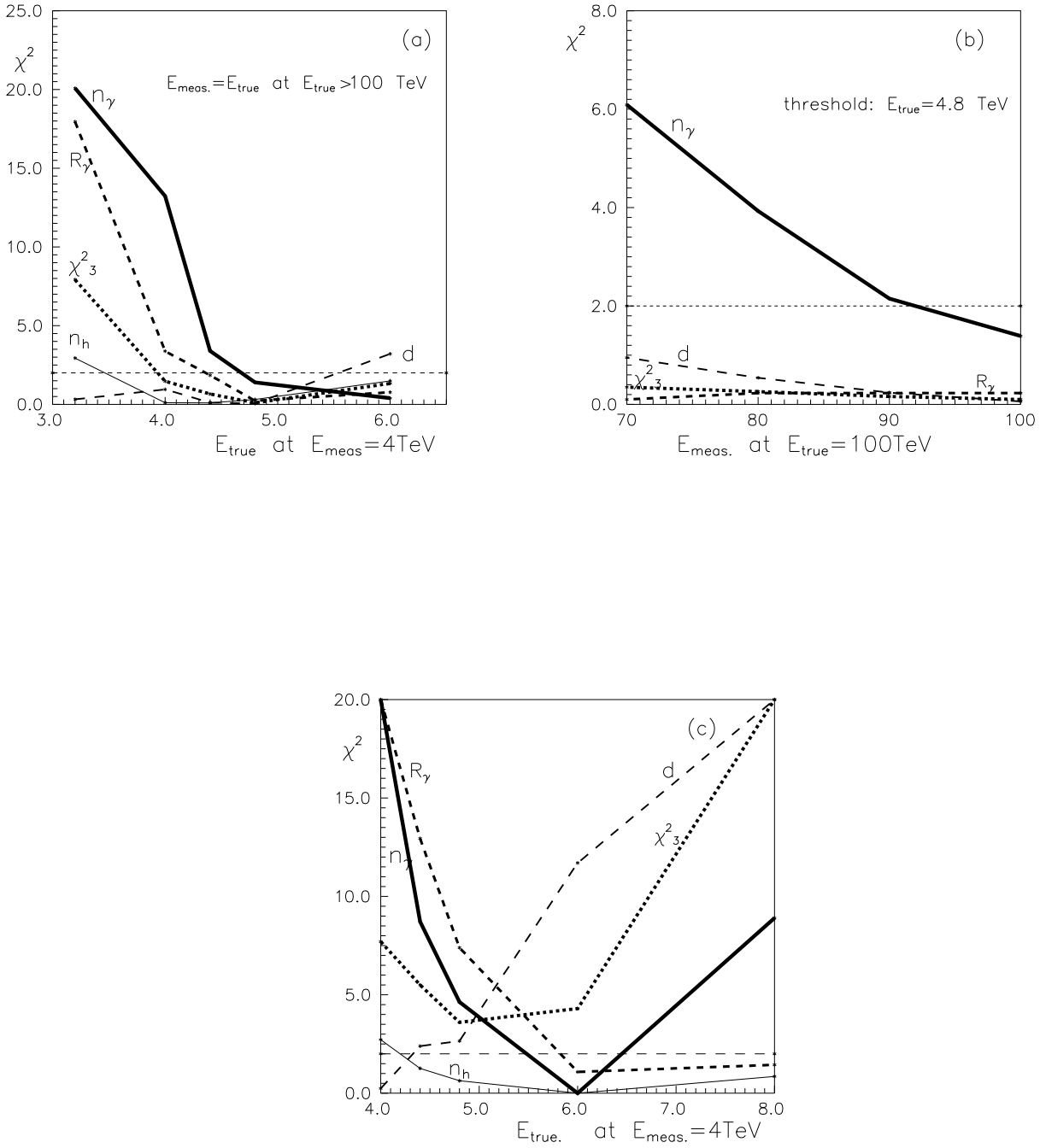

FIG. 9: Dependencies of χ^2_P and χ^2_3 on: a) degree of energy underestimation near measured threshold 4 TeV at normal chemical composition, b) degree of energy overestimation near true energy 100 TeV at normal chemical composition , c) the same as a) for heavy CC.

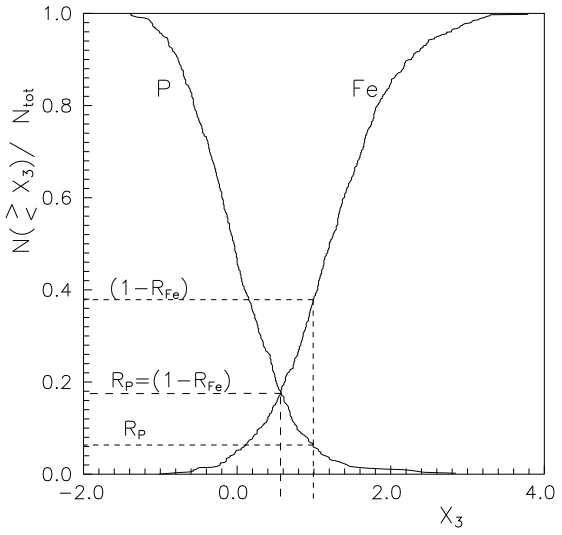

FIG. 10: Integral distributions of X_3 for families, generated by protons and iron. Limited values of X_3 correspondent to conditions $R_P = R_{Fe}$ and $R_P = 5\%$, are shown by dashed lines.